Metallophysics and Advanced Technologies
Металофіз. новітні технол.
Metallofiz. Noveishie Tekhnol.
2025, vol. 47, No. 1, pp. 57–81
https://doi.org/10.15407/mfint.47.01.0057
Reprints available directly from the publisher

PACS numbers: 46.25.-y, 46.35.+z, 81.20.Hy, 81.40.Gh, 81.40.Jj, 81.40.Lm, 83.60.Jk

Study of the Stress–Strain State of the Material of the Blanks during Plastic Stamping by Rolling

V. M. Mykhalevych, M. A. Kolisnyk*, and A. A. Shtuts*

Vinnytsia National Technical University,
95 Khmelnytske Shose,
21021 Vinnytsia, Ukraine
**Vinnytsia National Agrarian University,*
3 Sonyachna Str.,
21008 Vinnytsia, Ukraine

The work is aimed at solving an urgent problem in the scientific and technical field: the development and implementation of new technological processes in metal processing aimed at resource-saving and increasing production efficiency. Spinning is an important process in modern industry for the production of thin-walled workpieces, which are widely used in various industries. Investigation of the stress–strain state of the material during spinning is of great importance for improving manufacturing technologies and increasing product quality. This work proposes solutions of key research aspects such as the influence of process parameters (temperature, deformation rate, pressure, *etc.*) on the stress–strain state of the material. The relationship between these parameters and the mechanical properties of the processed material, including strength, plasticity, and crack resistance, is analysed. The investigation includes experimental methods such as mechanical testing, microstructural analysis, and modelling of deformation processes.

Key words: metal processing, spinning, resource-saving, technological processes, production efficiency, low-waste technologies, pressure material processing, stress–strain state, metal plasticity, forming, technological inheritance, complex-profile products.

Corresponding author: Volodymyr Markusovych Mykhalevych
E-mail: vmykhal2@gmail.ua

Citation: V. M. Mykhalevych, M. A. Kolisnyk, and A. A. Shtuts, Study of the Stress–Strain State of the Material of the Blanks during Plastic Stamping by Rolling, *Metallofiz. Noveishie Tekhnol.*, **47**, No. 1: 57–81 (2025). DOI: 10.15407/mfint.47.01.0057

Робота стосується вирішення актуальної проблеми в науково-технічній галузі: розробки та впровадження нових технологічних процесів металооброблення, спрямованих на ресурсозбереження та підвищення ефективности виробництва. Формування є важливим процесом промисловости для виробництва тонкостінних заготовок, які широко застосовуються в різних галузях промисловости. Дослідження напружено-деформованого стану матеріялу під час формування має важливе значення для вдосконалення технологій виготовлення та підвищення якости продукції. У даній роботі запропоновано вирішення ключових аспектів дослідження, таких як вплив параметрів процесу (температури, швидкости деформації, тиску тощо) на напружено-деформований стан матеріялу. Проаналізовано зв'язок між цими параметрами та механічними властивостями оброблюваного матеріялу, зокрема міцністю, пластичністю та тріщиностійкістю. Дослідження включають експериментальні методи: механічні випробування, аналізу мікроструктури й моделювання процесів деформації.

Ключові слова: металооброблення, формування, ресурсозбереження, технологічні процеси, ефективність виробництва, маловідходні технології, пресове оброблення матеріялів, напружено-деформований стан, пластичність металу, технологічна спадковість, вироби складного профілю.

(Received 8 May, 2024; in final version, 20 November, 2024)

1. INTRODUCTION

Spinning, as a process of forming metal workpieces, is of significant importance in modern industry, especially in the production of parts where the requirements for quality and precision are high.

Due to wide application of it and constant strive for optimizing production processes, research of the stress–strain state of the material during spinning becomes highly important. Understanding the internal processes occurring during material processing allows for the improvement of manufacturing technologies and the enhancement of product quality.

The object of the research is the behaviour of the material under the influence of various stamping parameters, such as temperature, deformation rate, pressure, and material thickness.

The analysis of the stress–strain state methods in spinning processes (SP) in the development and improvement of processes is particularly important. Information about the stress–strain state (SSS) of workpiece material and the influence of various technological processes on it allows determining the force parameters, evaluating the deformability of workpiece material, the stability of tooling, purposefully expanding the technological capabilities at the development stage, and predicting the operational characteristics of products. The most objective results are obtained from the study of SSS of workpiece material

using various research methods.

Due to the complexities of forming workpieces by SP method due to the influence of numerous factors, it is most expedient to use various experimental and computational methods for analysing SSS of the material.

Hardness measurement method. The hardness of a material is directly related to the maximum stress intensity experienced by the material throughout its entire history of plastic deformation σ_i [9, 12, 15]. Moreover, elastic unloading during cyclic deformation of metals does not lead to a change in hardness.

Therefore, the definition σ_i according to the results of the hardness measurement, it is possible only for cases of plastic deformation. Thus, for pressure treatment processes, it is possible to determine the intensity of stresses in the plastic zone based on the results of hardness measurements σ_i and taking into account the hypothesis of a single flow curve and intensity of deformations ε_i.

When investigating products obtained by SP method, the most suitable method for hardness measurement is the Vickers method, which provides a minimal plastic zone around the indentation. The use of the hardness measurement method requires the availability of a calibration chart for 'stress intensity–hardness–degree of deformation' σ_i–HV–ε_i.

Grading graphs of metals processed by rolling stamping (SHO) methods are built based on the results of hardness measurements on a hardness tester in the cross-sections of cylindrical samples deposited under conditions of a linear stress state. At the same time, the values are determined σ_i and ε_i according to the results of measuring the size of the samples and the deposition force according to the formulas:

$$\sigma_i = 4P / \pi d^2,\ \varepsilon_i = \ln(h_0 / h), \quad (1)$$

where P is deforming force, d is diameter of the deformed sample; h_0 and h are the height of the sample before and after deformation.

Samples are cut in the meridian direction, placed in a holder, and filled with epoxy resin. After hardening, the samples in the holder are ground using a series of abrasive papers, polished, and hardness is measured at 10–15 points of the cross-section. According to average hardness values and calculated values, σ_i and ε_i build grading graphs.

Figure 1 shows the workpieces obtained by SHO method according to the combined scheme of planting and reverse extrusion, cut, poured into a holder, polished and processed by measuring hardness with the construction of hardness isolines. Isolines of stress intensity and deformation intensity were obtained with the use of the constructed grading schedule based on them.

In Figures 2 and 3, grading graphs of M06 copper and low-alloyed steels 30ХГСА and 40ХН2МА are constructed, respectively. Of particular interest is the gradation graph of M06 copper, which has a

Fig. 1. Cross-sections of workpieces for hardness measurement.

strong dependence of stress intensity on strain intensity up to the values of the latter $\varepsilon_I \geq 1$. This allows determining the deformation intensity with sufficient accuracy based on hardness measurement results up to relatively high values. Thus, copper can be used for physical modelling of SP processes of other metals.

For the investigation of particularly thin-walled elements, the hardness measurement method is unsuitable due to the small size of the investigated plastic zone compared to the size of the indenter impression. Therefore, microhardness measurement of the material is used to analyse the strengthening of these zones μHV compared to the hardness measurement method, determining stressed deformed state (VAT) of the plastic zone by microhardness measurement is associated with a number of difficulties. First, when measuring the hardness, the imprint of the pyramid repeatedly overlaps various structural components that have different hardness. In the case of a homogeneous material, as a result of the measurements, the value of the average hardness is obtained, which depends only on the strengthening.

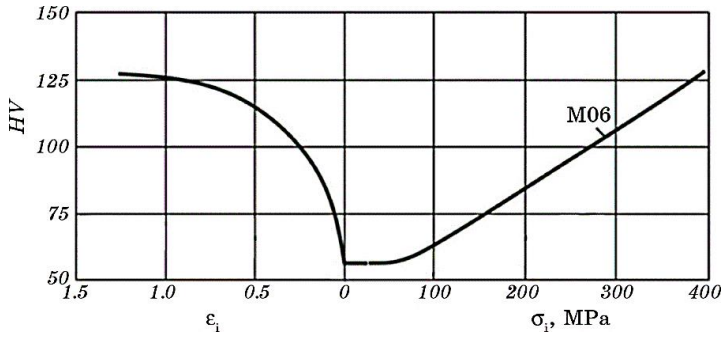

Fig. 2. Graduation graph σ_i–HV–ε_i copper M06.

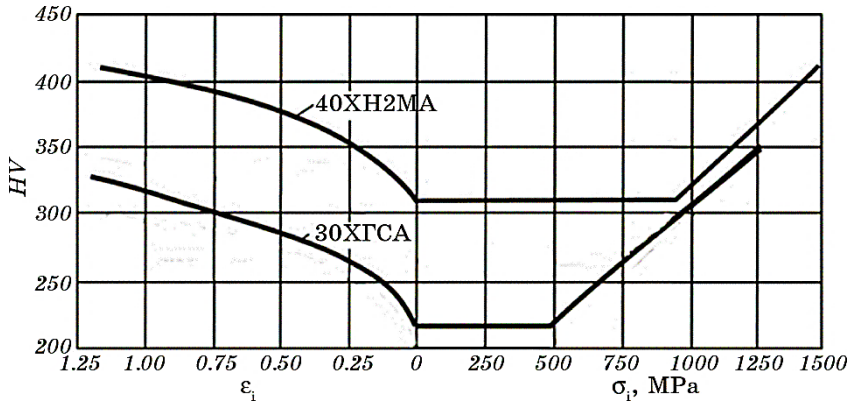

Fig. 3. Graduation graphs σ_i–HV–ε_i low-alloy steels.

When measuring microhardness, the size of the imprint, as a rule, does not exceed the size of a separate structural component. Therefore, to obtain reliable data, it is necessary to measure the microhardness in the same structural component, preferably in the one that strengthens the most. This is not always possible, especially if you need to get information in the form of an array of values in some area.

On the other hand, since the hardness is related to the microhardness of the structural components, this relationship can be represented in the form of certain dependence [14]. In work [18, 20] the specified dependence is adopted in the form of a linear model:

$$H = H_1 a_1 + H_2 a_2 + C, \tag{2}$$

where a_1, a_2, C are constants that do not depend on ε_i.

Thus, the microhardness of the structural components can be converted into the macrohardness of the material and obtain an already substantiated dependence.

On the other hand, if there is strengthening in the workpiece with the same degree, then the study SSS can be carried out by direct measurement of microhardness. For this, it is necessary to collect only statistics of microhardness values μHV at every level.

Our research showed that, if we make about 15 measurements of microhardness in a zone with the same degree of hardening, we would get its average value, which clearly correlates with the values σ_i and ε_i. At the same time, there is no need to monitor the microhardness of any individual structural component. Study of the regularity of the distribution of values σ_i and ε_i in the deformed layer by measuring microhardness in work [20, 21, 25] confirm the effectiveness of this method.

To build grading graphs σ_i–HV–ε_i samples are used, as for measuring hardness. However, surface preparation for microhardness meas-

urement is significantly different, as even a slight defamation of the surface layer distorts the measurement results. While measuring the hardness, the riveted thin layer is pressed by the pyramid and does not affect noticeably the hardness reading.

When investigating SSS of the plastic zone in blanks obtained by spin forming methods, they are cut and the surface is prepared similarly to the surface of calibration samples. Measurements of hardness are then conducted at intervals that prevent the overlapping of plastic zones from indenter impressions. By analysing the hardness measurements of the deformed zone and using calibration graphs, isoclines of distribution are obtained σ_i and ε_i. When necessary, the accuracy of the results obtained on specific sections (usually near the free surface of the blank) is verified using the grid method. Within the scope of conducted research, this method was used to determine SSS of the plastic zone in blanks during direct and reverse extrusion by the spin-forming method. Figure 4 depicts a holder with prepared polished sections of copper blanks, spun to various degrees according to a combined scheme of embossing with reverse extrusion.

The slip line field method. Based on the construction of a slip line field that meets static and kinematic boundary conditions, the distributions of stresses, strain rates, and the magnitude of accumulated strain along the flow lines, as well as the stress state index, are determined:

$$\eta = I_1(T_\sigma) / \sqrt{3I_2(D_\sigma)}\ , \qquad (3)$$

where $I_1(T_\sigma)$ is the first invariant of the stress tensor, $I_1(D_\sigma)$ is the second invariant of the stress deviator.

The obtained results of the research on SSS of the billet allow us to determine the energy and force parameters of the process, the amount

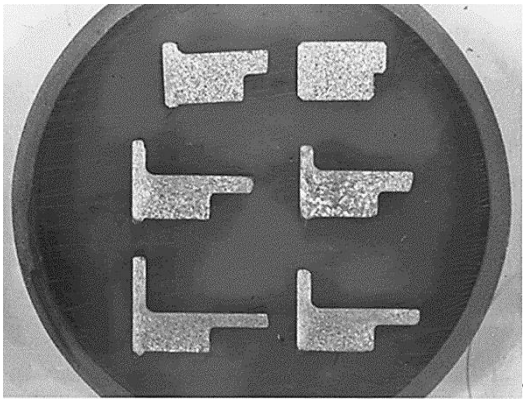

Fig. 4. Appearance of the holder with polished sections of copper blanks, prepared for microstructural analysis and hardness measurement.

of used plasticity resource of the metal, and the quality parameters of the produced products. This method was developed for the conditions of studying rolling processes.

The grid method. It belongs to the most common experimental-calculative method for determining SSS of deformed billets. Changes in co-ordinate-dividing grids allow determining the components of deformation at different stages of the deformation process. For the first time, it is obtained the ratio for calculating deformations based on distorted square dividing grids [1, 2, 10]. Renne generalized the method for the case, when the initial cell has the shape of a parallelogram.

Using this research methodology, studies can be conducted by measuring the co-ordinates of nodes step by step, *i.e.*, determining the fields of displacements over a certain period of time, followed by determining the fields of deformation rates. The stress state is calculated based on the deformed state using the relationships of plasticity theory. In this case, the stress field must satisfy the equilibrium equations, plasticity conditions, flow law, and boundary conditions.

The most commonly used approach is one in which the task of calculating the kinematics of deformation based on the known co-ordinates of nodes of the distorted dividing grid is reduced to constructing approximations $X(X_0, Y_0, t)$, $Y(X_0, Y_0, t)$ co-ordinates of nodes $\tilde{X}_{l,n}, \tilde{Y}_{l,n}$ grids (where X_0, Y_0 are Lagrangian variables associated with the undeformed sample) and their derivatives in co-ordinates and time. In this approach, the type of approximations used plays an important role. An approach, in which spline functions of one argument or a combination of splines of one argument (by time) and splines of two arguments (by co-ordinates at each stage) are used for approximation, and differentiation has become widespread. At the same time, the more effective approach, from the point of view of the accuracy of the approximation, is the approach in which the time derivatives of the co-ordinates of the nodes are first calculated (that is, the flow velocities of the material particles), and then their derivatives in terms of co-ordinates X_0, Y_0.

When studying spin-forming methods, the grid method needs to consider two types of heterogeneous input information: analytical and geometric. Analytical information consists of differential and algebraic equations that the unknown functions in the plastic domain and at its boundary must satisfy. Geometric information concerns the shape of the boundary of this domain. A fairly effective approach in studying metal forming processes using the grid method is the method of specifying geometric information and its calculation when constructing differential relationships using the theory of R-functions [21, 22, 25].

A function of several arguments is called an R-function if it changes sign only when at least one of its argument's changes sign. The following system of R-functions is most commonly used:

$$x \wedge y = x + y - \sqrt{x^2 + y^2},\ x \vee y = x + y - \sqrt{x^2 + y^2},\ \neg x = -x. \qquad (4)$$

The operations in formulas (4) are called R-conjunction, R-disjunction, and R-negation. It is obvious that R-conjunction is positive only in the first quadrant, while R-disjunction is positive in the first, second, and fourth quadrants.

An equation of the domain Ω and its boundary Γ is called an equation of the form:

$$\omega(x, y) = 0, \qquad (5)$$

if $\omega_\Gamma = 0$ i $\omega > 0$ inside the domain and $\omega < 0$ outside it. For clarity in constructing equations of domains, one can consider R-conjunction as the intersection of domains, and R-disjunction as their union.

The calculation of geometric information in analytical expressions in the R-functions' method is carried out using the concept of the solution structure of the problem, which is why the R-functions' method is also called the structural method. Let $U(x, y)$ be an unknown field in a certain domain Ω, which is a solution to a variational problem under certain conditions on the boundary Γ

$$L_{iU} = R_i \text{ in } \Gamma_i (i = \overline{1, m}) \qquad (6)$$

and in the region

$$A_U = V, \qquad (7)$$

where A and L_i are known differential or functional operators, V and R_i are known functions.

The structure of the solution to problem (6), (7) is called the following form:

$$U \equiv B(\varphi_1, \ldots, \varphi_n, \varphi), \qquad (8)$$

which for any sufficiently smooth functions will identically $\varphi_i(x, y)$ satisfy (6), (7). The correct and converse statement: for any function U satisfying (6), (7) $\varphi_1, \ldots, \varphi_n$ can be found such that (8) holds, then (8) is a complete structure. Proof of the completeness of structures is in general a difficult problem, and often the proof of completeness is the successful results of numerical experiments.

The functions $\varphi_1, \ldots, \varphi_n$ in formula (8), as shown in [11–14], are conveniently applied using finite functions, such as Shenberg B-splines. The presented methodology allows working with irregular and non-rectangular grids in areas with any shape of boundaries, and is also suitable for many transient processes where different grids are applied

at different transitions.

The finite element method (FEM) is a generalization of the variational method and belongs to the effective modern methods that allow determining the stress–strain state of inhomogeneous media [17, 18].

Considerable experience has been accumulated in the investigation of metal forming processes using numerical methods to determine the stress–strain state through direct variational methods, particularly the Ritz method, which equates the work of external and internal forces and has been further developed in works [3, 6, 7, 9], among others. The use of FEM significantly overcomes the difficulties in selecting coordinate functions and utilizes the capabilities of variational methods to determine not only integral but also local characteristics of the processes of plastic strengthening of machine part surfaces.

FEM is an effective numerical method for solving a wide range of boundary problems in continuum mechanics. It involves replacing the object under study with a set of discrete elements interconnected by nodes. The direct transition to the computational formula allows for naturally forming boundary conditions and arbitrarily placing the nodes in the element grid.

The most significant advantages of FEM in addressing metal forming processes include the freedom to choose nodal points, the arbitrary shape of the workpiece, the ability to set any necessary boundary conditions, considering the heterogeneity of material properties, and the use of standard software programs.

In the context of technological calculations, the sequence of solving a non-stationary nonlinear plasticity problem using FEM consists of the following steps [20, 22, 23]: problem formulation, discretization scheme, computation and result visualization procedure on a computer.

The problem formulation involves a mathematical description of the deformation schemes. To simplify the mathematical model, assumptions about the material property changes are introduced, namely, the material of the part is modelled as an elastoplastic material, friction coefficients between the workpiece and the tool are constant, and the tool is modelled as an absolutely rigid body.

The mathematical model also includes auxiliary equations that determine contact interaction, friction forces, and the condition of volume constancy. In modelling metal forming operations (MFO), the condition of volume constancy must be maintained, meaning the model's elements must also be of constant volume. In FEM, the compressibility of each element is characterized by a stiffness coefficient. This implies that the compressibility of any part of the workpiece-tool system, represented by a matrix of stiffness coefficients of its elements, ensures that elements only change their configuration during deformation without decreasing in volume.

The independent parameters are the nodal variables, and the distri-

butions within the elements are determined through them. As unknown kinematic and thermodynamic quantities, there are chosen-nodal velocities and displacements [7, 8, 20, 21].

The simplest form of idealization for a two-dimensional problem involves using triangles with nodes located at the vertices. These elements were among the first used.

Reducing the size of elements improves the convergence of FEM significantly more than increasing the order of elements. The reasons for this are: the influence of nodal variables is most pronounced when nodal points coincide with the vertices of elements, which is best facilitated in linear elements where all nodes lie at the vertices, from the second criterion of convergence, it follows that reducing the size of elements always leads to an increase in the accuracy of the solution due to better convergence, analysis of high-speed, nonlinear, and non-stationary MFO processes requires breaking the workpiece into small elements in areas with large gradients and abrupt changes in metal flow.

2. PRESENTATION OF THE MAIN RESEARCH MATERIAL

The most development and usage have been gained by the processes of orbital forging (OF) for obtaining complex profiled parts by implementing radial material flow of cylindrical workpieces using schemes of upsetting, flanging, spreading, squeezing, *etc*. Additionally, for a number of workpieces, a complex profile of the end part is characteristic, which can be obtained through direct extrusion (half-couplings are presented in Fig. 5, *a*, thrust bearing rings are presented in Fig. 5, *b*, *etc*.) [2].

Direct extrusion by OF method can be implemented in a rolling die with the necessary profile on the end of the workpiece opposite the end

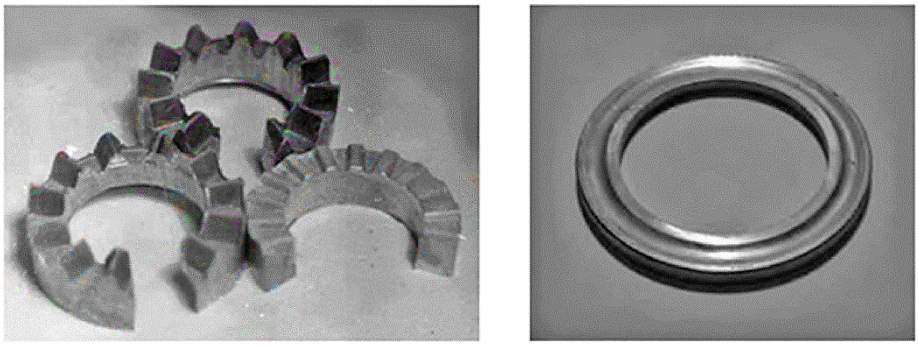

a *b*

Fig. 5. Workpieces obtained by OF method: cam half-couplings at different stages of rolling (*a*), thrust bearing ring (*b*).

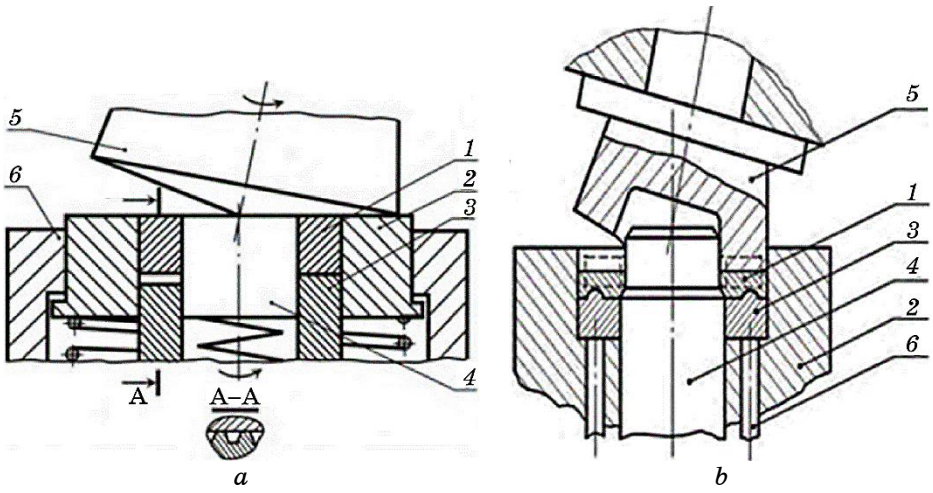

Fig. 6. Technological schemes of direct extrusion of the profile on the end of the workpiece by OF method: in a spring-loaded die and mandrel (*a*), in the die calibre of the stamp (*b*).

contacting the roll.

Figure 6 illustrates the technological schemes of forming and the corresponding elements of the workpiece ends.

Insufficient research of this process does not contribute to the development of technological schemes with a specified flow of material and the formation of necessary elements of the product. The lack of information about the material workability of the workpiece prevents the assessment of deformability and determination of the technological capabilities of the process based on factors of workpiece material failure and tool durability. The technological inheritability of the obtained products also remains undefined. Therefore, the study of the workability of workpiece materials is one of the important factors in improving processes of stamping by extrusion [1, 2]. To establish the influence of various technological parameters on the workability of the material, experimental research methods were initially applied: the method of hardness measurement, the method of dividing grids, and the analysis of the materials' microstructure.

The application of these methods in this work allows constructing paths of material particle deformation in the critical zones of the workpiece, which are used to assess the materials' deformability.

For physical modelling of the direct extrusion process by the extrusion method, the ring workpiece consists of two rings: internal and external. A rectangular dividing grid was applied to the external cylindrical surface of the internal ring. The appearance of the deformed rings, with a portion of the external ring cut off, is shown in Fig. 7.

Fig. 7. View of the rings after direct extrusion of the end profile by the extrusion method and cutting off a part of the external ring.

Figure 8 shows the view of the deformed grid on the surface of the internal ring at the initial (*a*), intermediate (*b*), and final (*c*) stages of direct extrusion by the extrusion method.

Figure 9 presents view of the deformed grid on the external surface of the punch.

When physically modelling the direct extrusion processes using elements skin (EC) method, copper M06 and armco-iron were chosen as

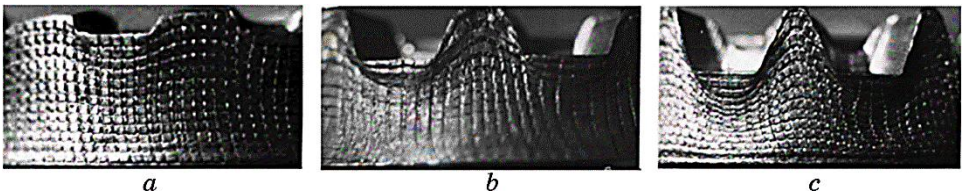

Fig. 8. View of the deformed mesh on the outer surface of the inner ring at different stages of direct extrusion by EC method.

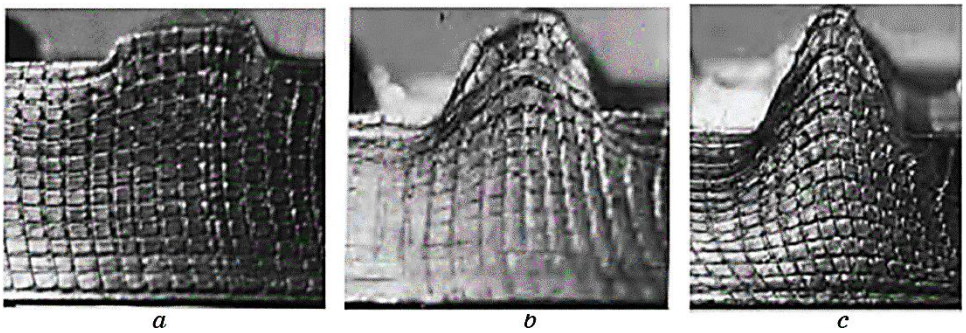

Fig. 9. View of the deformed mesh on the outer surface of the punch at different stages of direct extrusion by EC method.

the workpiece materials. Copper is characterized by high strengthening during plastic deformation, allowing for the precise determination of the distribution of deformation intensity in the internal zones of the workpieces with a high degree of accuracy. It also exhibits a pronounced but non-uniform initial microstructure. Armco-iron has a uniform grain structure, which can complement the results of the study with a microstructural analysis.

The view of the deformed microstructure of the copper M06 material in the cross-section of the punch at intermediate and final stages of deformation is shown in Fig. 10. Figure 11 presents an enlarged view of the microstructure of copper M06 at characteristic points (corresponding to Fig. 10, *b*) of the formed profile.

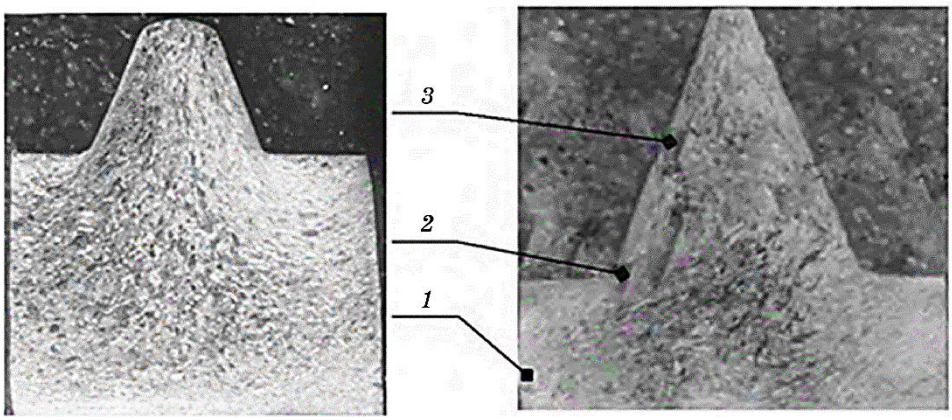

Fig. 10. View of the deformed microstructure of the workpiece material made of copper M06 in the cross-section of the punch at intermediate and final stages of deformation.

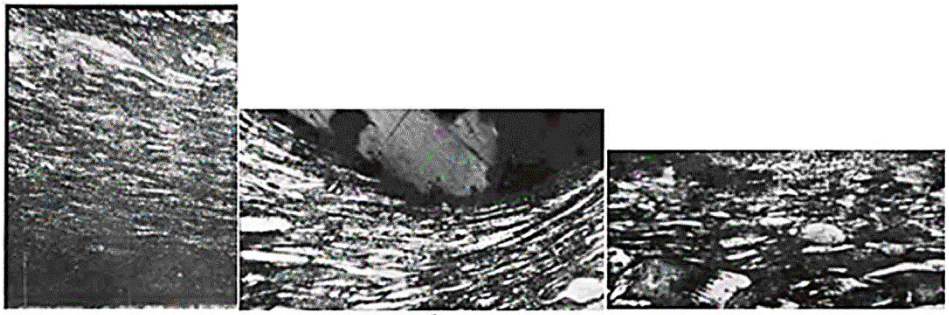

Fig. 11. Magnified view of the workpiece microstructure at characteristic points of the formed profile corresponding to Fig. 10, *b*: point *1* (contact zone with the roller) (*a*), point *2* (*b*), point *3* (*c*).

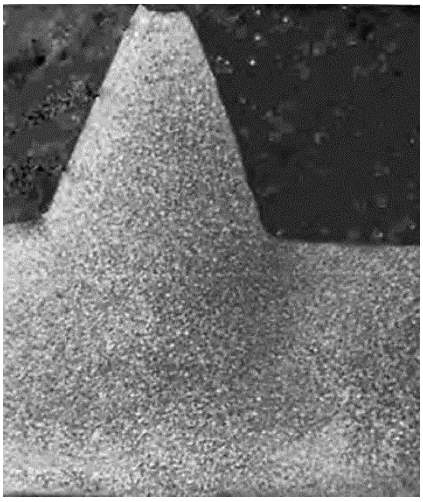

Fig. 12. View of the deformed microstructure of the workpiece material made of armco-iron in the cross-section of the die at the final stage of deformation.

The workpiece made of armco-iron (see Fig. 12) has a fine-grained structure, which was studied for individual zones under significant magnification.

The hardness measurement method is an effective way to determine the stress intensity σ_i in the workpiece without prior separation. Therefore, for processes of direct extrusion using the method, the stress intensity σ and the deformation intensity ε_i can be determined in the plastic zone of the workpiece based on hardness measurement results, taking into account the hypothesis of a single yield curve.

The graduation curve of copper M06 is shown in Fig. 2.

The investigation of the workpiece materials' nonuniform deformation state (SSS) by the hardness measurement method was conducted according to the technique presented in [3]. Figure 13 shows the distribution of deformation intensity in the extruded element zone obtained by hardness measurement.

Thus, the distribution of the intensity of deformations in the zone of the extruded element (see Fig. 12), obtained by the hardness measurement method, indicates a rather uneven nature of the deformed state in the cross section of the workpiece. The greatest intensity of deformations, which is observed in the contact zone of the roll with the workpiece, reaches the values $\varepsilon_I = 0.9–1.0$ and may exceed them. The next, most deformed, is the zone of entry of the metal into the forming channel. Here, the intensity of deformations reaches values $\varepsilon_I = 0.6–0.7$. The lowest level of deformations is observed at the free top of the extruded element and in its central part, and the intensity of deformations here reaches values $\varepsilon_I = 0.1–0.2$.

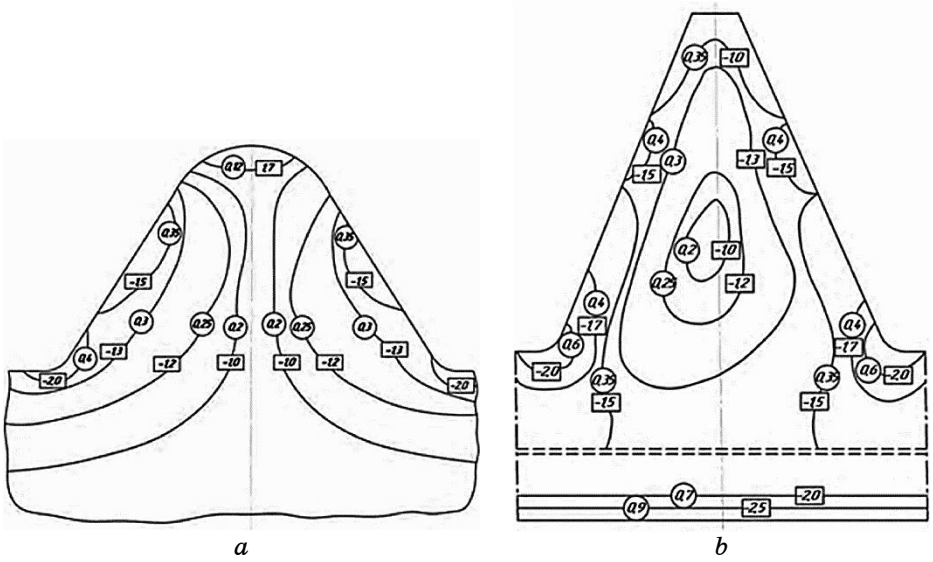

Fig. 13. Distribution of VAT parameters in the workpiece element obtained by extrusion using SHO method at intermediate (*a*) and final (*b*) stages: (O)η = const and (Ω)ε_i = const.

To study SSS of the plastic zone of the workpiece during direct extrusion by SHO method, we also used the method of co-ordinate dividing grids, built on the use of a technique based on the theory of *R*-functions [1]. At the same time, step-by-step extrusion of the element was carried out (see Fig. 8): a flat task. Character of distribution of isolines ε_I = const within the zone of the extruded element obtained from the results of the measurement of the co-ordinate dividing grid is shown in Fig. 14.

Thus, the distribution of the deformed state, obtained by the method of co-ordinate grids, coincides with that obtained by hardness measurement. The stress index in the zone of maximum deformation is $\eta = -2.5 \dots -2.0$ (see Fig. 13). These conditions indicate the presence of significant compressive stresses here, which makes the deformability of the blank material relatively safe. However, there is a risk of tooling failure in the areas near the tooth base. The material of the blank at the tooth tip undergoes relatively small deformations, but the stress index here is that requires an assessment of $\eta > +1$ material's deformability.

An important feature of this technological scheme is that metal particles from the free tooth tip and the 'stiff' stress scheme, during extrusion, come into contact with the tool, where their deformations continue to increase under the 'soft' stress scheme ($\eta = -1.3 \dots -1.5$). All this must be taken into account when constructing paths of material deformation to assess its deformability.

Another characteristic of the deformation is that, as can be seen in

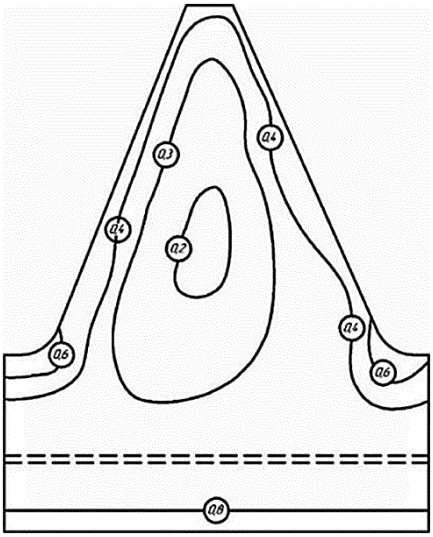

Fig. 14. Distribution of deformation intensity in the plane of the punch extruded by EC method, obtained from the measurement results of the coordinate grid.

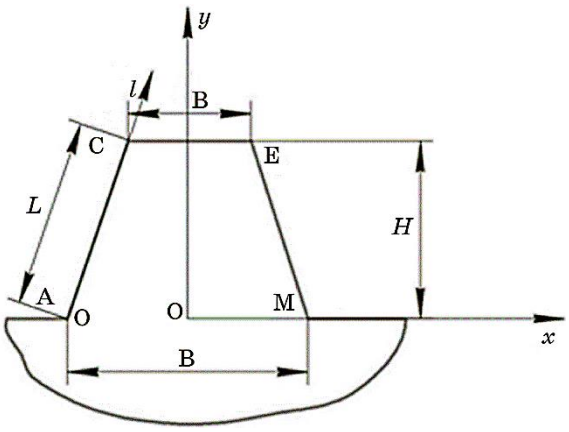

Fig. 15. Characteristic parameters of the profile of the element extruded by EC method.

Figs. 9 and 13, the deformation pattern in relation to the profile of the extruded element has a certain asymmetry. This is due to the asymmetric application of the load during blanking. Such a flow pattern is useful if the side surfaces of the element have different inclination angles. If it is necessary to eliminate the noted asymmetry, it is advisable to consider reversing the blank.

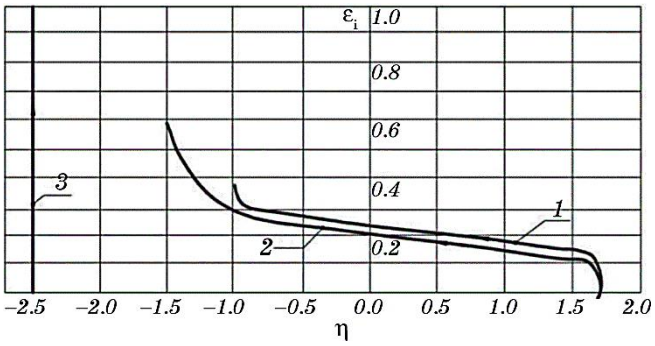

Fig. 16. Deformation paths of the material particles in the most characteristic deformed zones: in the middle of the lateral surface AC (*1*), at the entrance to the forming channel (near point A) (*2*), in the contact zone of the blank with the mandrel (*3*).

When changing the parameters of the element profile, characterized by the values shown in Fig. 15, the values of deformation intensity and stress index will change somewhat, but the character of their distribution will remain the same. The distribution character of the noted quantities will also remain unchanged when changing materials if the friction conditions remain unchanged.

To assess the deformability of the blank material and determine the limiting deformations, from the point of view of preventing material failure or ensuring the necessary technical characteristics of the part, it is necessary to have paths of deformation of particles in dangerous zones. Figure 16 shows the paths of deformation of particles of the blank material in the most deformed zones, obtained by the method of co-ordinate grids using the theory of *R*-functions.

The peculiarity of the deformation paths lies in the fact that at the initial stage of extrusion, the material on the line OM undergoes stretching at a stress ratio of $\eta = 1.73$. At the same time, the magnitude of deformation intensity is relatively small, reaching values of $\varepsilon_I = 0.15–0.20$ for the free surface at the final stage of shaping.

Subsequently, upon contact with the lateral surface of the matrix channel, deformation continues under conditions of $\eta = -1.0–+1.5$. For the most deformed area in contact with the mandrel, the deformation path *3* can be represented by an average value of the η parameter of $\eta = -2.5–-2.0$ in the mandrel pressure zone.

The extrusion scheme shown in Fig. 17, *a* provides for the extrusion of the flange and the reverse extrusion of the thin-walled element, and is implemented with a positive displacement of the apex of the conical mandrel (see Fig. 17, *a*). By displacing the apex of the mandrel along the axis of the blank, the flow of the flange material inside the blank can be ensured.

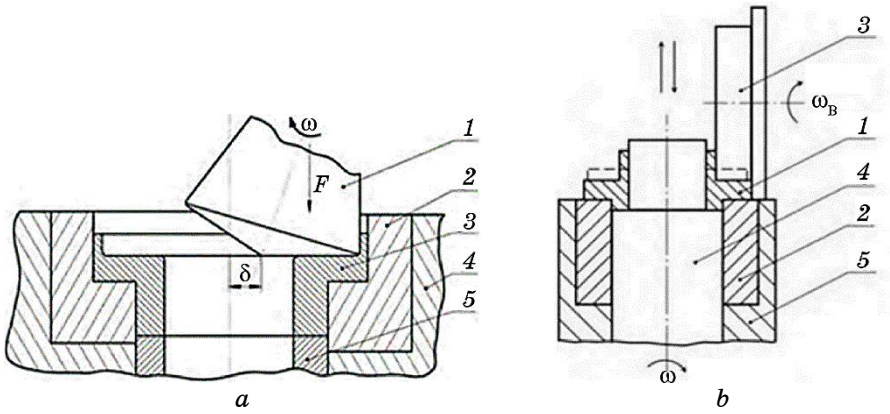

Fig. 17. Schemes of extrusion and reverse extrusion of thin-walled elements by SHS method on the end face of a ring blank with conical (*a*) and cylindrical (*b*) mandrels: *1*—blank, *2*—matrix, *3*—mandrel, 4—pusher sleeve, *5*—spindle.

The extrusion scheme shown in Fig. 17, *b* provides for the extrusion of the flange and the reverse extrusion of the thin-walled element, and is implemented with a negative displacement of the axis of the cylindrical mandrel (see Fig. 10).

To enhance the processes, an analysis of the residual stress distribution (RSD) in the blank material was conducted during the operations of both flanging and reverse extrusion using SSS method.

Figure 18 presents isolines of stress intensity distribution $\sigma_I = \text{const}$ and deformations $\varepsilon_I = \text{const}$, which were obtained from the results of measuring the hardness in the cross-sections of the blanks at different stages of rolling (the corresponding sections are shown in Fig. 4).

Thus, in the cross-section of the blank formed at the first stage of rolling (Fig. 18, *a*), the following characteristic zones of residual stress distribution can be identified.

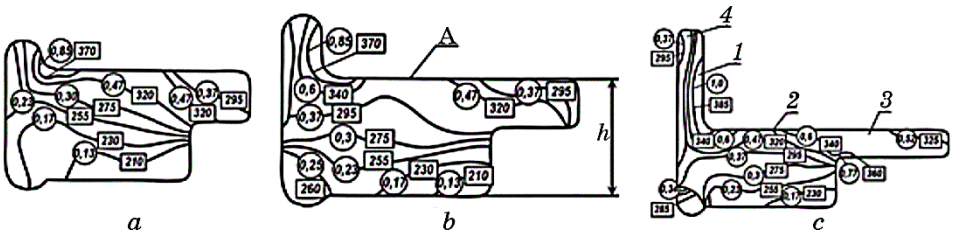

Fig. 18. Distribution of isolines (O)η = const and (Ω)ε_i = const in the cross-sections of M06 copper ring blanks formed by severe plastic deformation method.

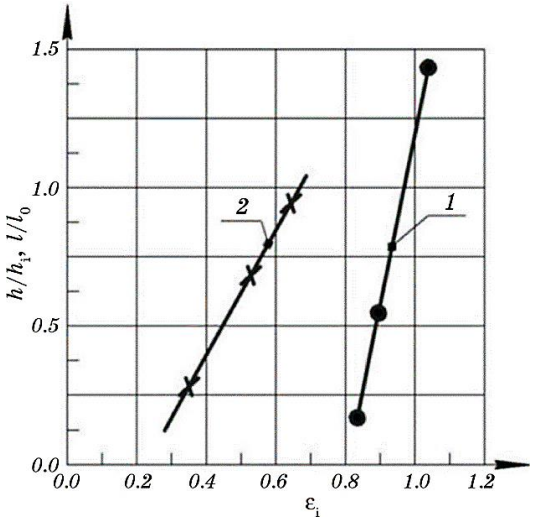

Fig. 19. Dependency of the relative height change of the thin-walled element h/h_i on the maximum intensity of deformations (*1*), and the relative size of the flange l/l_0 on the intensity of deformations in its peripheral area (*2*), according to Fig. 18.

The most deformed is the zone of the thin-walled element *1*, which is formed because of metal flow from zone *2*. The minor further deformation of zone *1*, as the height of the thin-walled element increases, (Fig. 19, dependence *1*) occurs due to successive cyclic shifts in the axial direction, caused by the characteristics of local loading in severe plastic deformation, and the increased resistance to metal flow in the gap between the roll and the mandrel.

Zone *2*, where the highest degree of deformation is observed at the contact with the roll (surface A), which gradually decreases as it moves away from the contact surface. The metal from zone *2* (Fig. 18, *b*) flows into zones *1* and *3*, and the intensity of its flow in one direction or another depends on the relative positioning of the roll and the blank [1, 3].

Zone 3 (the flange part of the blank) is a zone of relatively uniform deformation. The increase in deformation intensity on the periphery of the flange, depending on the relative increase in its length, is depicted in Fig. 19 by line *2*.

The distribution of the stress state index along the arc of contact in the middle part of the flange and along the contour of the blank formed by the roll is presented in Fig. 20. Thus, in the area with the highest intensity of deformations, a stress state pattern is observed that approximately corresponds to biaxial compression ($\eta \cong -2.0$).

Use of metals with higher resistance to plastic deformation σ_s, as well as an increase in unit crimping Δh leads to an increase in the stress

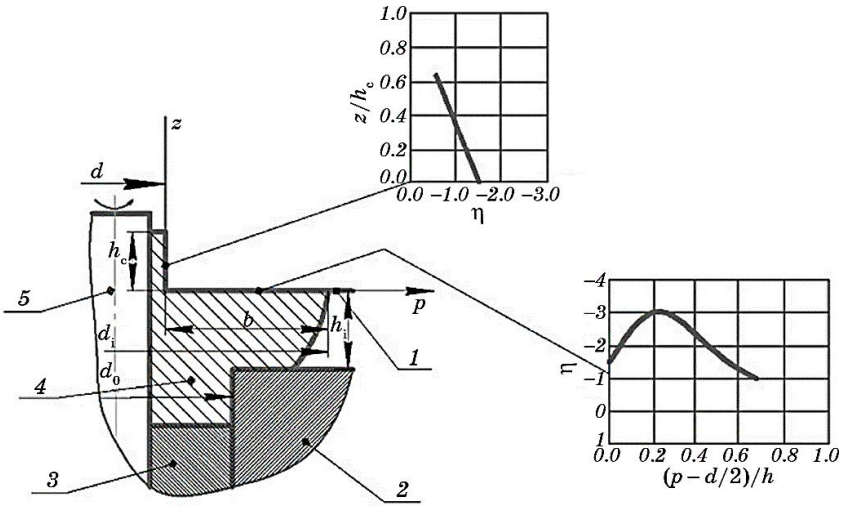

Fig. 20. Distribution of the stress state index along the height of the thin-walled element and along the width of the flange.

level, but does not have a noticeable effect on the indicator η.

It should be noted that in the zone of formation of maximum deformations in the thin-walled element there is a 'soft' scheme of the stress state ($\eta < -1.5$).

A stiffer stress state occurs in the flange part of the workpiece, namely on the peripheral, free from contact with the tool, surface (see Fig. 20).

Therefore, the assessment of the deformability of the workpiece material to determine the maximally achievable intensity of deformations ε_* or the value of the plasticity resource used ψ_B, should be carried out specifically for this zone.

Figure 21 shows the paths of deformation of metal particles on the free surface of the flange during its extrusion, depending on the parameters of the extrusion process.

Thus, the most favourable paths in terms of deformability are those with minimal ratio of deformed height to wall thickness of the workpiece and negative displacement of the roller tip.

Therefore, knowing the main parameters of the workpiece and its position during orbital forging, such as h_0, b_0 and δ, we can analytically describe the paths of metal deformation on the dangerous external surface of the flange and use this to assess the workpiece material's deformability.

Figure 22 shows graphs illustrating the patterns of change in the possible stress state values with increasing plastic deformation, depending on the parameters of the constructed model.

Stress state index η as a function of parameters θ and m at different

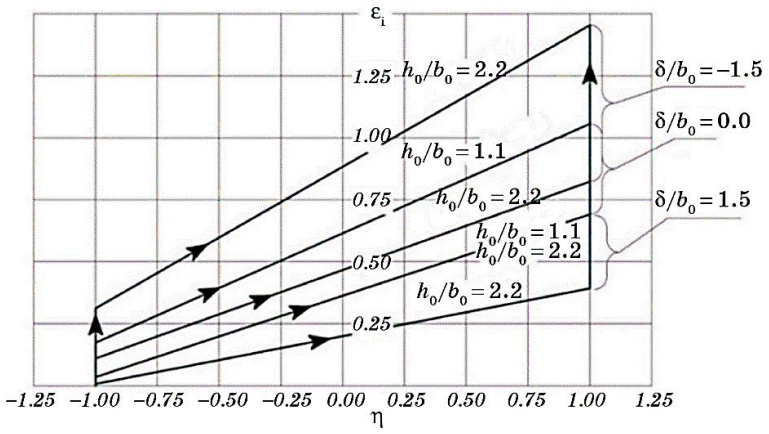

Fig. 21. Paths of deformation of the free surface of the peripheral part of the flange during orbital forging (h_0, b_0 are initial height and wall thickness of the tubular workpiece to be coined, δ is displacement of the tip of the conical roll from the axis of the workpiece).

stages of plastic deformation calculated using (9):

$$\begin{cases} \eta(t) = \dfrac{\dfrac{3}{2}(4-(1+\theta)(1+3\cos^2 t))}{\sqrt{9+\dfrac{3}{4}(2-(1+\theta)(1+3\cos^2 t))^2}}, \\ \bar{e}_i(t) = \dfrac{\sqrt{3}}{6} m \displaystyle\int_0^t \frac{\sqrt{(2-(1+\theta)(1+3\cos^2\tau))^2+12}}{\cos^2\tau}\, d\tau, \end{cases} \tag{9}$$

$$m \in [0,\infty), \theta \in [0,1], t \in [0, \pi/2].$$

Note that the last relation has only one material constant m, and the generalized relation (9) has two material constants: θ, m.

Another advantage of the recently derived relationship is the absence of a material constant in the analytical expression for the stress state in the parametric representation of deformation trajectories.

This leads to additional conveniences in analysing these relationships and selecting the material constant based on experimental data. In the generalized relationships (9), the material constant m is also absent in the analytical expression for the stress state indicator, although another material constant remains θ. These drawbacks are a natural trade-off for the ability to develop a more adequate model for the change in the stress state of a macro-particle of material on the free surface of the blank during roll stamping, given the displacement of the cone roller's apex from the blank's axis towards the contact spot.

Figure 23 presents the deformation trajectories we have constructed

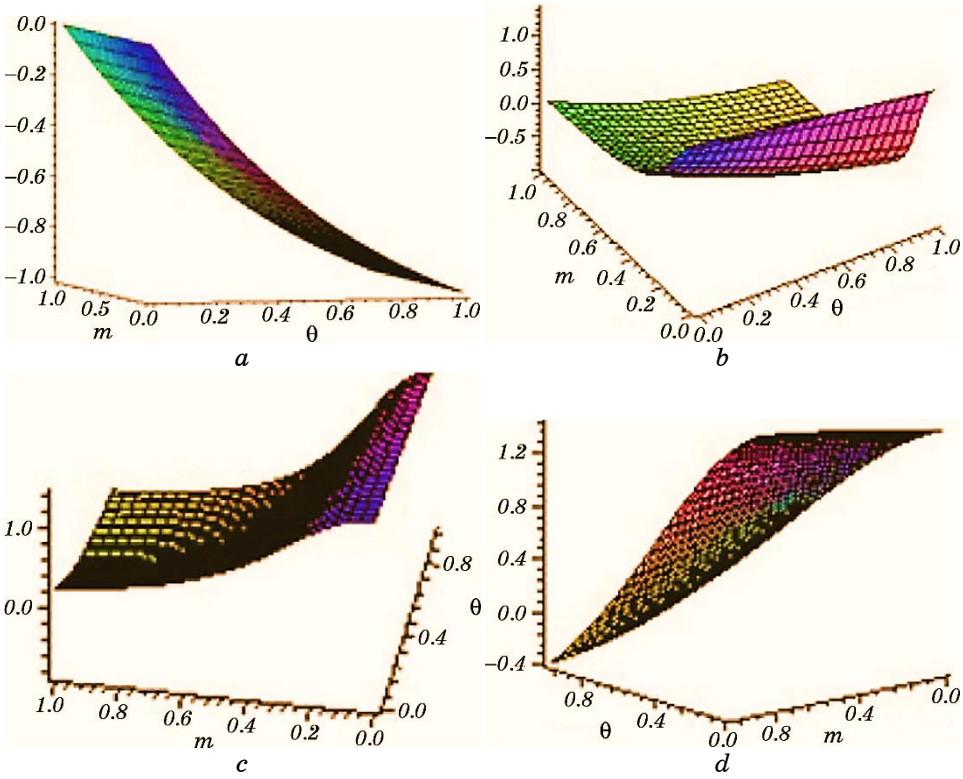

Fig. 22. Paths of deformation of the free surface of the peripheral part of the flange during orbital forging (h_0, b_0 are initial height and wall thickness of the tubular workpiece to be coined, δ is displacement of the tip of the conical roll from the axis of the workpiece).

for different values of material constants θ and m.

The advantages of representing deformation trajectories as parametric equations include the ease of analysing these trajectories. For instance, with a fixed value of the constant θ, we can determine the value of the parameter t that corresponds to the point, where the deformation trajectory intersects the y-axis. Based on the first equation of set (10), we can write

$$\eta(t) = 4 - (1 + \theta)(1 + 3\cos^2 t) = 0,\ t \in [0, \pi / 2], \tag{10}$$

from which follows

$$t = \arccos\left(\sqrt{\frac{3 - \theta}{3(1 + \theta)}}\right). \tag{11}$$

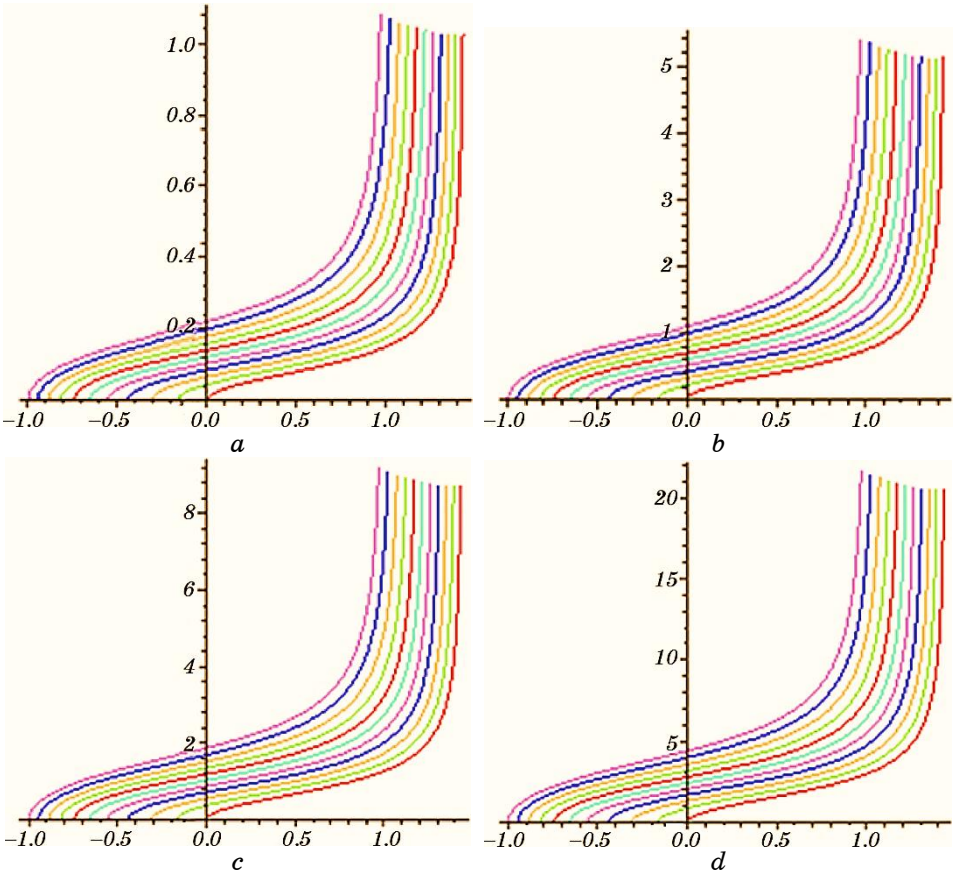

Fig. 23. Deformation trajectories $\bar{e}_i = \bar{e}_i(\eta)$ calculated for (10): $\theta \in [0, 1]$, $m =$ 0.1 (*a*), 0.5 (b*)*, 0.85 (*c*), 2.0 (*d*).

For example, at $\theta = 1$, $t \cong 0.9553166180$. Based on the second equation of system (12), we determine

$$\frac{\bar{e}_i(t = 0.9553166180)}{m} = \int_0^{0.9553166180} \sqrt{3 + \frac{1}{\cos^4 t}}\, dt \approx 2.206. \qquad (12)$$

From the last equality, it is easy to determine the ordinate (the amount of accumulated deformation) of the point of intersection of the deformation trajectory with the ordinate axis, in particular,

$$\bar{e}_i(\eta = 0, m = 0.1) \approx 0.22,\ \bar{e}_i(\eta = 0, m = 0.5) \approx 1.1,$$
$$\bar{e}_i(\eta = 0, m = 0.85) \approx 1.88,\ \bar{e}_i(\eta = 0, m = 2.0) \approx 4.41. \qquad (13)$$

3. CONCLUSION

The stress–strain state of workpiece material is an important characteristic necessary for assessing deformability and determining force parameters. Among the effective methods of NDS analysis are the grid method, hardness measurement, and microstructural analysis.

Direct extrusion by SHO method was considered by us using the example of forming end teeth of a gear sleeve. To increase the accuracy of determining deformation intensity in cross-sections of workpieces, a highly strengthening material—copper M06 was chosen for physical modelling.

As a result of constructing graduation graphs and measuring hardness in workpiece cross-sections, as well as grids on workpiece surfaces, the distribution character of stress and strain intensity, as well as the stress state index in the plastic area, was obtained. The most rigid stress state scheme is observed at the apex of the extruded teeth, but here the least deformation occurs. The largest deformations are formed at the base of the tooth, but the stress state is close to uniaxial compression.

Reverse extrusion by SHO method was also modelled on copper M06. NDS analysis showed that the most deformed zone is the thin-walled element zone, which is formed because of metal flow from the contact plastic spot area of the roller with the workpiece. Maximum deformations are observed in this zone, gradually decreasing as you move away from the contact surface. The flange part of the workpiece is a zone of relatively uniform deformation. Dependences of the growth of deformation intensity on the periphery of the flange from the relative increase in its length were constructed.

Based on the analysis results, paths of material particle deformation in dangerous zones due to possible workpiece destruction were constructed, which were then used to assess workpiece material deformability.

The possibilities of direct extrusion are limited by the complexity of force transmission from the roller to the opposite end face of the workpiece and significant contact stresses. Therefore, this operation is more suitable for calibration or forming of small-sized workpiece elements, which should be taken into account when developing corresponding SHO technological processes.

Further research in this direction will expand knowledge of material deformation mechanisms during stamping by extrusion and develop new approaches to optimizing technological processes in the production of metal parts.

REFERENCES

1. V. A. Matviychuk, *Tekhnika, Ehnergetyka, Transport APK*, No. 4: 110 (2022) (in Ukrainian).
2. A. A. Shtuts', *Herald of Khmelnytskyi National University. Series: Technical*

Sciences, **235**, Iss. 2: 167 (2016) (in Ukrainian).
3. A. A. Shtuts' and V. A. Matviichuk, *Tekhnika, Ehnergetyka, Transport APK*, No. 3: 178 (2016) (in Ukrainian).
4. V. A. Matviichuk, M. A. Kolysnyk, and A. A. Shtuts', *Tekhnika, Ehnergetyka, Transport APK*, No. 3: 77 (2018) (in Ukrainian).
5. A. A. Shtuts' and M. O. Sluzhaliuk, *Vibratsiyi v Tekhnitsi ta Tekhnolohiyakh*, No. 2: 138 (2020) (in Ukrainian).
6. A. A. Shtuts', *Vibratsiyi v Tekhnitsi ta Tekhnolohiyakh*, No. 4: 101 (2020) (in Ukrainian).
7. I. Kupchuk, M. Kolisnyk, A. Shtuts, and M. Paladii, *Bulletin of the Transilvania University of Braşov. Series I: Eng. Sci.*, **14**, No. 2: 1 (2021) (in Romania).
8. A. Shtuts and M. Kolisnyk, *Agricultural Eng.*, **54**: 62 (2022).
9. V. Matviychuk and A. Shtuts, *Traditional and Innovative Approaches to Scientific Research : Theory, Methodology, Practice* (Riga: Baltija Publishing: 2022), p. 90.
10. V. A. Matviichuk, V. M. Mykhalievych, and M. A. Kolysnyk, *Vibratsiyi v Tekhnitsi ta Tekhnolohiyakh*, No. 1: 81 (2022) (in Ukrainian).
11. V. A. Matviichuk and V. M. Mykhalievych, *Development of Local Deformation Processes: Theory and Practice of Pressure Treatment of Materials* (Zaporizhzhia: Motor Sich: 2016), p. 339 (in Ukrainian).
12. V. M. Mikhalevich, A. A. Lebedev, and Y. V. Dobranyuk, *Strength Mater.*, **43**: 591 (2011) (in Ukrainian).
13. A. A. Lebedev and V. M. Mikhalevich, *Strength Mater.*, **35**: 217 (2003).
14. V. O. Kraievskyi, V. A. Matviichuk, and V. M. Mykhalievych, *Improvement of Processes and Equipment for Pressure Treatment in Mechanical Eengineering and Metallurgy* (Kramatorsk–Sloviansk: 2003), p. 286 (in Ukrainian).
15. N. S. Hrudkina, O. E. Markov, A. A. Shapoval, V. A. Titov, I. S. Aliiev, P. Abhari, and K. V. Malii, *FME Trans.*, **50**, No. 1: 90 (2022).
16. V. Dragobetskii and A. Shapoval, *Metallurgical and Mining Industry*, No. 4: 363 (2015) (in Ukrainian).
17. V. Sikulskiy, V. Kashcheyeva, Y. Romanenkov, and A. Shapoval, *Eastern-European J. Enterprise Technol.*, **4**, No. 1: 43 (2017).
18. V. Dragobetskii, A. Shapoval, E. Naumova, S. Shlyk, D. Mospan, and V. Sikulskiy, *Proc. Int. Conf. Modern Electrical and Energy Systems MEES (November 15–17, 2017, Kremenchuk)* (IEEE: 2018), p. 400.
19. I. Kupchuk, M. Kolisnyk, A. Shtuts, M. Paladii, and A. Didyk, *Colloquium-Journal*, No. 16: 40 (2021).
20. S. Gundebommu, V. Matvijchuk, O. Rubanenko, and Yu. Branitskiy, *Mater. Today: Proc.*, **38**: 3337 (2021).
21. V. Matvijchuk, A. Shtuts, M. Kolisnyk, I. Kupchuk, and I. Derevenko, *Periodica Polytechnica, Mech. Eng.*, **66**, No. 1: 51 (2022).
22. O. L. Gaidamak, *Tekhnika, Ehnergetyka, Transport APK*, No. 4: 90 (2022) (in Ukrainian).
23. O. Gaidamak, *Tekhnika, Ehnergetyka, Transport APK*, No. 2: 161 (2022) (in Ukrainian).
24. V. Matviychuk, O. Gaidamak, and M. Karpiychuk, *Vibratsiyi v Tekhnitsi ta Tekhnolohiyakh*, No. 2: 65 (2022) (in Ukrainian).
25. M. Pulupec and L. Shvets, *Current Problems of Transport*, 195 (2019).
26. E. Posviatenko, N. Posviatenko, R. Budyak, L. Shvets, Y. Paladiichuk, P. Aksom, I. Rybak, B. Sabadash, and V. Hryhoryshen, *Eastern-European J. Enterprise Technol.*, **5**. No. 12: 48 (2018).